Cesium Azide—An Efficient Material for Green Light-Emitting Diodes With Giant Quantum Dots

Hoang-Tuan Vu, Chun-Yuan Huang, Chih-Jung Chen, Ray-Kuang Chiang, Hsin-Chieh Yu, Ying-Chih Chen, and Yan-Kuin Su, *Fellow, IEEE*

***Abstract*— A novel efficient and air-stable electron injection layer (EIL) of cesium azide (CsN_3) was compared with conventional ones including CsF, Cs_2CO_3, LiF and without EIL in type-II quantum dot light-emitting diodes (QLEDs) with both organic electron and hole transport layers. Via directly decomposing to pristine cesium (Cs), the low-temperature evaporated CsN_3 provided a better interfacial energy level alignment without damaging the underneath organic layer. Consequently, the current efficiencies of 7.45 cd/A was achieved in the CsN_3-based green QLEDs consisting of giant CdSe@ZnS/ZnS quantum dots at 544 nm, which was 310% (at 10 mA/cm^2) improvement over the LiF-based QLEDs. Moreover, the light turn-on voltage in CsN_3-devices significantly decreased ∼5.5 V in comparison with LiF-devices.**

***Index Terms*— Quantum dots (QDs), quantum dot light-emitting diodes (QLED), cesium azide (CsN_3), electron injection, alkali metal compound.**

I. Introduction

RECENTLY, the quantum dots (QD) light-emitting diodes (QLEDs) is becoming a promising candidate for high-efficiency and color-saturated displays because of their numerous superior advantages, such as pure color, high CRI, and band gaps/emission tunability [1]–[3]. As previously reported, four types of device architectures were classified based on the charge transport materials being organic or inorganic [2]. Due to the band edge mis-alignment of colloidal II-VI QDs and those well-used anode and cathode materials-indium tin oxide (ITO) and Al, the importance of charge transport layers has been extensively demonstrated and new functional materials are being explored [3]. For type-II QLEDs, the use of both organic hole transport layer (HTL) and electron transport layer (ETL) harvests all advantages of organic and polymer LEDs while possessing robust quantum dot emission [2]. However, organic charge transport layers cause large energy barriers with sandwiched QD emission layer, which leads to poor injection efficiency in such organic/QD/organic architecture. Conditions become worse when QDs with higher band gaps are adopted to reach green or blue emission. To solve the problem, Ho et al. utilized the polymer small molecule mixture (poly-N-vinylcarbazole (PVK): 20 wt % 4,4′,4″-tris(N-carbazolyl)-triphenyl-amine (TCTA)) as organic HTL leading to a great enhancement in current efficiency [4]. Also, Bae et al. introduced a nanohybrids film containing green QDs and a hole conducting polymer poly(4-butyl-phenyl-diphenyl-amine) (poly-TPD), so as to suppress the phenomenon of efficiency roll-off to achieve stable EQE ∼1.4% at current density below 200 mA/cm^2 [5]. In a similar way, organic ETL such as 1, 3, 5-tris (2-N-phenylbenzimidazolyl) benzene (TPBi), tris(8-hydroxyquinoline)aluminum (Alq_3) and 2,9-dimethyl-4,7-diphenyl-1,10-phenanthroline (BCP) were used in QLEDs to reduce the energy barrier [6], [7]. However, those organic ETLs with better energy level alignment for electron transporting into QDs inevitably increase the injection barrier and decrease the mobility for electrons from Al cathode. Being an effective solution, a buffer such LiF or CsF acting as electron injection layer (EIL) is capable to overcome above drawbacks. By applying LiF as EIL with QD-conducting polymer nanohybrid, the maximum luminance can reach ∼ 6500 cd/m^2 [5]. In this letter, several well-developed electron injection materials in organic devices were evaluated and compared in type-II QLEDs for the first time.

II. Experimental Process

The green CdSe@ZnS/ZnS QDs were synthesized according to the method previously reported [8]. In a typical synthesis, cadmium oleate (0.07 mmol), zinc oleate (1.705 mmol), oleic acid (OA) (3.1 mL), and 1-octadence (ODE) (7.5 mL) were mixed in a 100 mL three-neck flask and degassed at 310 °C under N_2 flow. An anionic stock solution was prepared by dissolving Se (1 mmol) and S (1 mmol) in trioctylphosphine (TOP) (1.5 mL). Then, Se-S-TOP (1.5 mL) was injected into the above hot mixture to grow the composition gradient-shell CdSe@ZnS QDs. For ZnS shell coating, S (0.8 mmol) dissolved in ODE (1.2 mL)

Manuscript received April 20, 2015; revised June 23, 2015; accepted July 6, 2015. Date of publication July 10, 2015; date of current version September 14, 2015. This work was supported by the Ministry of Science and Technology, Taiwan, under Contract MOST 103-2221-E-006-001. *(Corresponding authors: Chun-Yuan Huang and Yan-Kuin Su.)*

H.-T. Vu, H.-C. Yu, and Y.-C. Chen are with the Advanced Optoelectronic Technology Center, Department of Electrical Engineering, Institute of Microelectronics, National Cheng-Kung University, Tainan 701, Taiwan (e-mail: vhtuan87@gmail.com; hcyu@mail.ncku.edu.tw; tnwo.m1812@msa.hinet.net).

C.-Y. Huang is with the Department of Applied Science, National Taitung University, Taitung 950, Taiwan (e-mail: laputa@nttu.edu.tw).

C.-J. Chen and R.-K. Chiang are with the Nanomaterials Laboratory, Far East University, Tainan 74448, Taiwan (e-mail: liver08@ms58.hinet.net; rkc.chem@msa.hinet.net).

Y.-K. Su is with the Advanced Optoelectronic Technology Center, Department of Electrical Engineering, Institute of Microelectronics, National Cheng-Kung University, Tainan 701, Taiwan, and also with the Department of Electrical Engineering, Kun-Shan University, Tainan 710, Taiwan (e-mail: yksu@mail.ncku.edu.tw).

This letter has supplementary downloadable material available at http://ieeexplore.ieee.org., provided by the authors. The material is 622 KB in size.

Color versions of one or more of the figures in this letter are available online at http://ieeexplore.ieee.org.

Digital Object Identifier 10.1109/LPT.2015.2454052

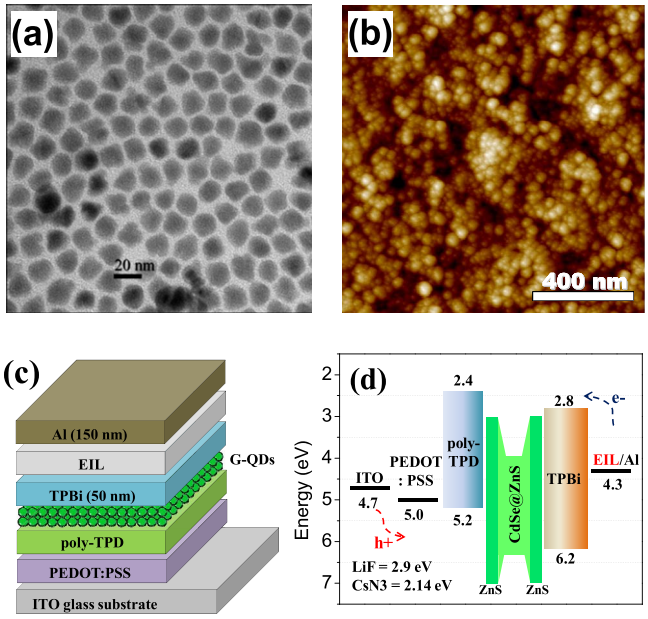

Fig. 1. (a) TEM and (b) AFM images of giant CdSe@ZnS/ZnS QDs coated on a copper grid and a poly-TPD layer, respectively. (c) Schematic of device structure and (d) energy band diagram of QLEDs with different EILs.

was introduced into the above CdSe@ZnS QD solution and the reaction was kept for 12 minutes. Next, a mixture of zinc acetate dihydrate (1.43 mmol), OA (0.5 mL), and ODE (2 mL) was injected at 310 °C and the temperature was immediately reduced to 270 °C. Then, a S stock solution dissolving S (4.825 mmol) in TOP (2.5 mL) was added dropwise at a rate of 0.25 mL/min, and the additional ZnS shelling proceeded for 20 minutes. The resulting CdSe@ZnS/ZnS QDs were precipitated by adding excess ethanol and repeatedly washed; finally, the purified QDs were redispersed in hexane. The resulting CdSe@ZnS/ZnS QDs were precipitated by adding excess ethanol and repeatedly washed; finally, the purified QDs were redispersed in hexane. The surface ligand of synthesized QDs was exchanged as 1-dodecane-thiol (DDT) to increase the quantum yield (QY) to 65% [9]. Based on previous definition, the colloidal QDs with shell thickness larger than ten monolayers are called "giant" QDs [10]. Being the giant QDs with thick composition-gradient-shell to suppress the Auger recombination [8], the size of green CdSe@ZnS/ZnS QDs is around 13-16 nm, as indicated in the transmission electron microscopy (TEM) image (Fig. 1(a)). Energy-dispersive spectroscopy result shows that the atomic contents of Cd, Se, Zn, and S are 4%, 14.6%, 58.6%, and 22.8%, respectively. In device fabrication, patterned ITO-glass substrates were cleaned with DI water, acetone, and 2-propanol, respectively, and treated with UV-zone for 25 minutes. Subsequently, a 40-nm-thick poly(3,4-ethylenedioxythiophene): poly(styrenesulfonate) (PEDOT:PSS) and a 30 nm-thick poly-TPD layers were spin-coated onto the substrates, respectively. The QD emission layer was then deposited from the QD-hexane solution (10 mg/ml). Without apparent aggregations or clusters, the atomic force microscopy (AFM) image of the QD layer shown in Fig. 1(b) exhibited a roughness of 3.7 nm. Samples were transferred to a vacuum chamber (1×10^{-6} torr) to evaporate a 50-nm-thick

TABLE I
SUMMARY OF ALL GREEN QLEDS

Sample	Light turn-on voltage (V)	L_{max} (cd/m^2)	(cd/A)	EQE_{max} (%)
w/o EIL	18.1	2547	2.52	0.75
LiF	11.5	837	2.38	0.76
Cs_2CO_3	11	2875	3.35	1.05
CsF	9.3	1524	4.30	1.47
CsN_3	5.8	12400	7.45	2.30

TPBi ETL at a deposition rate of ~0.1 nm/s. Finally, different EILs of CsN_3 (3 nm), LiF (0.6 nm), Cs_2CO_3 (3 nm), and CsF (3 nm) were respectively deposited and followed by a Al cathode (150 nm) as shown in Fig. 1(c). The active areas of 1×1.2 mm^2 were defined by using shadow masks during organic and metal evaporation process. After fabrication, the devices were preserved and characterized in a nitrogen-filled glove box using a Keithley 2400 source-meter, a Keithley 2000 multi-meter, a silicon photo-detector and a PR650 colorimeter.

III. RESULTS AND DISCUSSION

For better understanding of the carrier injection, the energy band diagram of our QLEDs are schematically shown in Fig. 1(d) according to previous reports [6], [11]. In type-II QLEDs, thickness and uniformity of ETL can be well-controlled with a smoother surface in contact with EIL to avoid current crowding and local joule heating. In this device configuration, the capability of alkali metal compounds to reduce the main barrier between TPBi and Al is an important factor to improve performance of QLEDs besides the barrier in HTL/QD interface. In OLED-related studies, it is fully acceptable that the capability for electron injection of these compounds strongly depends to these very thin alkali metals or alkali sub-oxides films such as Li, Cs_2O, and Cs which are liberated from decomposing reaction during thermal evaporation [12]–[15]. These metals and compounds acting as the n-type dopants in contact with emission layer (EML) or ETL induces a larger energy bending and a smaller electron barrier to facilitate electron injection from cathode to EML. Similarly, it was reported that the electron barrier reduced from 0.71 to 0.15 eV without any interface dipole by adding a CsN_3 EIL between Alq_3/Al interfaces [12]. The current density-voltage (J-V) and luminance-voltage (L-V) curves of QLEDs are shown in Fig. 2 and some representative characteristics of five types of devices are listed in Table I. The light turn-on voltage of LiF-, Cs_2CO_3-, CsF-, and CsN_3-devices are 11.5, 11, 9.3, 5.8 V, respectively, compared with a value of 18.1 V in the device without EIL. The significant variations of light turn-on voltage in devices clearly demonstrate that the electron is the minority carrier for determination of light threshold. Holes are more easily injected than electrons in our device configuration. The performance improvement in Fig. 2 is typically attributed to the reduction of energy barrier by the decomposed Li, Cs_2O, Cs at the Al interface which present low work function (WF) of 2.9, 2.2, and 1.9 eV, in cases of LiF, Cs_2CO_3, and CsF/CsN_3, respectively [13]–[15]. We noticed

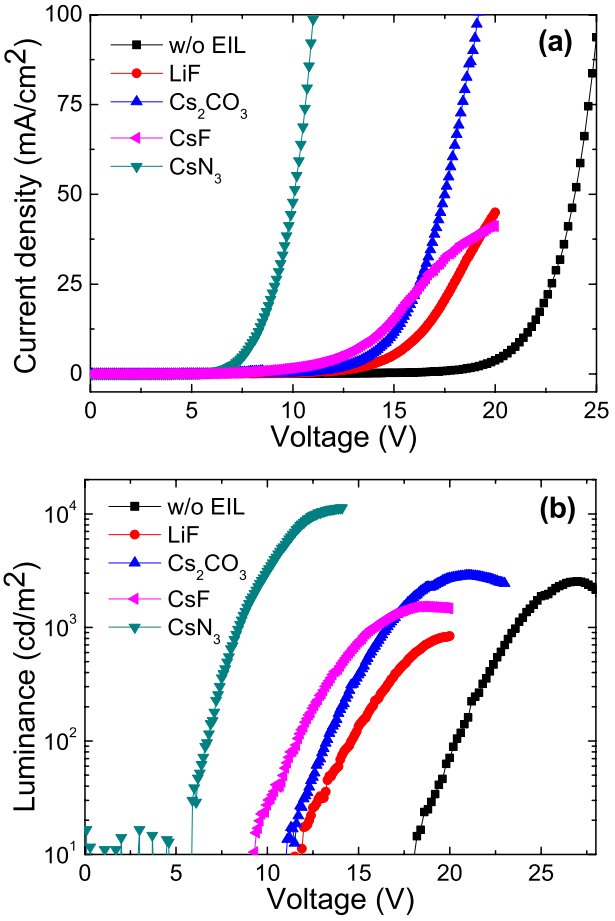

Fig. 2. (a) Current density-voltage ($J-V$) and (b) luminance-voltage ($L-V$) characteristics of QLEDs with different EILs.

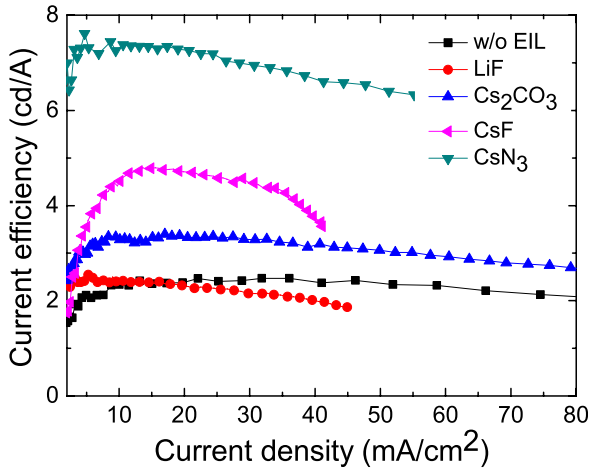

Fig. 3. Current efficiency-current density (η-J) characteristics of QLEDs.

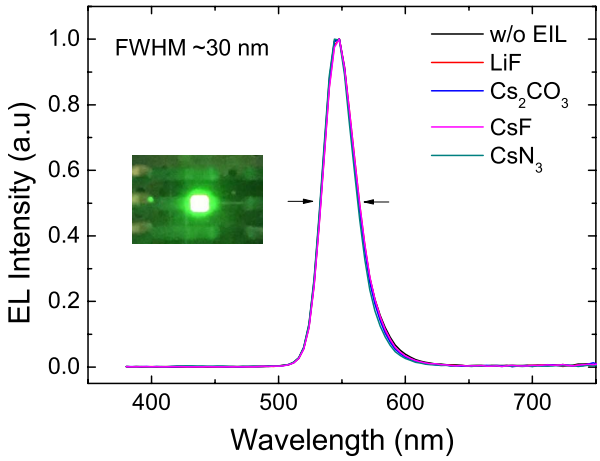

Fig. 4. EL spectra of QLEDs driven at 10 mA/cm^2. Inset is an emission image of CsN_3-devices.

that the melting temperature of CsN_3 was reported about 310 °C which was much lower than that of 850, 610 and 682 °C for LiF, Cs_2CO_3 and CsF, respectively. Therefore, lower evaporation temperatures also imply better and easier evaporating process besides the difference of liberated metals or compounds finally attached on TPBi. However, the considerable decrease ($>$ 6 V) in light turn-on voltage after the use of EILs may not entirely attributed to the reduction ($<$ 1.5 V) of energy barrier calculated based on previous reports. The positively-charged QDs and electric field build up should also be taken into account. It turns to be $\sim$ 50 % reduction of driving voltage (@ 10 mA/cm^2) from 15.8 (LiF-devices) to 8.0 V. The maximum luminance is also enhanced from 837 to 12400 cd/m^2. This result is easily appreciated since CsN_3 possesses a stronger electron-negativity to dope the ETL more readily. Despite Cs_2CO_3- and CsF-devices present better performances than LiF-device, they still have their own drawbacks to overcome, even though the exactly same Cs metals are dissociated in CsF- and CsN_3-devices. In CsF-devices, the rapid saturation of injection current may be explained by the instability and moisture absorbing in air during the evaporation of CsF. In Cs_2CO_3-device, the reported higher WF of Cs_2O ($\sim$2.2 eV) can be responsible for our findings [12], [14].

The current efficiency-current density (η-J) characteristics of the devices are illustrated in Fig. 3. Due to the limited minority carrier in LiF-device, the current efficiency can only reach 2.38 cd/A at 10 mA/cm^2 whereas η of 7.45 cd/A, corresponding a 310 % enhancement, is achieved in CsN_3-device. Since all devices have identical QD emitters with the same conditions (thickness and QY) and a presumably identical hole injection density at the same bias voltage, the current efficiency directly reflects the degree of carrier unbalance in QDs. The instability of CsF-device is also clearly observed according to the roll-off in current efficiency (adequate electron injection rate and sharp degradation). A maximum current density of only 40 mA/cm^2 (worse than the device without EIL) is achieved in CsF-devices; while the corresponding saturation of luminance and efficiency roll-off indicate that the electrons are limited at higher voltages. Statistically, the $\sim$40 and $\sim$80 % enhancements are exhibited in Cs_2CO_3- and CsF-devices with current efficiency of 3.35 and 4.3 cd/A compared with LiF-device. Besides, the maximum external quantum efficiency (EQE) as a function of current density for all devices is provided in Supplementary Information.

Normalized electroluminescence (EL) spectra of all QLEDs driven at current density of 10 mA/cm^2 are shown in Fig. 4. All EL spectra exhibit an identical emission peak at 544 nm and

a full-width at half maximum (FWHM) of ∼30 nm, without any emission signal from poly-TPD or TPBi. When applied voltage increase, the intensity of all QLEDs also increase consequently without any shift of the peak's position and the difference of FWHM values. Therefore, it can be concluded that the effective carrier recombination is only carried out in the QD layer. The inset of Fig. 4 shows an emission image of CsN_3-device driven at 10 mA/cm^2, and the emission corresponds to the CIE-1931 coordinates of (0.367, 0.624). To further extend the viability of CsN_3 in performance of QLEDs, the QLEDs with red CdSe/ZnS QDs were also fabricated and the results are given in Supplementary Information.

IV. Conclusions

We have proposed an efficient electron injection layer based on CsN_3 to fabricate type-II green QLEDs with giant CdSe@ZnS/ZnS QDs. Robust air-stability, low-temperature evaporation, and certain decomposition make CsN_3 an ideal electron injection material in QD-related applications. In our experimental results, low light turn-on voltage (∼ 5.8 V), high maximum luminance (12400 cd/m^2) and efficiency (7.45 cd/A) of green QLEDs were achieved with an emission peak at 544 nm. In characteristic comparison of CsN_3- and CsF-devices, though the pure Cs metals are supposed on ETLs, CsF-device is not as resistible as CsN_3-device against high current stress.

References

[1] J. Kwak *et al.*, "Bright and efficient full-color colloidal quantum dot light-emitting diodes using an inverted device structure," *Nano Lett.*, vol. 12, pp. 2362–2366, Apr. 2012.

[2] Y. Shirasaki, G. J. Supran, M. G. Bawendi, and V. Bulović, "Emergence of colloidal quantum-dot light-emitting technologies," *Nature Photon.*, vol. 7, pp. 13–23, Jan. 2013.

[3] X. Dai *et al.*, "Solution-processed, high-performance light-emitting diodes based on quantum dots," *Nature*, vol. 515, pp. 96–99, Nov. 2014.

[4] M. D. Ho, D. Kim, N. Kim, S. M. Cho, and H. Chae, "Polymer and small molecule mixture for organic hole transport layers in quantum dot light-emitting diodes," *ACS Appl. Mater. Inter.*, vol. 5, pp. 12369–12374, Oct. 2013.

[5] W. K. Bae *et al.*, "Reduced efficiency roll-off in light-emitting diodes enabled by quantum dot–conducting polymer nanohybrids," *J. Mater. Chem. C*, vol. 2, no. 25, pp. 4974–4979, Mar. 2014.

[6] K. S. Leck *et al.*, "Quantum dot light-emitting diode with quantum dots inside the hole transporting layers," *ACS Appl. Mater. Inter.*, vol. 5, pp. 6535–6540, Jun. 2013.

[7] B.-H. Kang *et al.*, "Enhanced charge transfer of QDs/polymer hybrid LED by interface controlling," *IEEE Electron Device Lett.*, vol. 34, no. 5, pp. 656–658, May 2013.

[8] K.-H. Lee *et al.*, "Over 40 cd/A efficient green quantum dot electroluminescent device comprising uniquely large-sized quantum dots," *ACS Nano*, vol. 8, no. 5, pp. 4893–4901, Apr. 2014.

[9] C.-J. Chen, R. K. Chiang, C.-Y. Huang, J.-Y. Lien, and S.-L. Wang, "Thiol treatment to enhance photoluminescence and electroluminescence of CdSe/CdS core-shell quantum dots prepared by thermal cycling of single source precursors," *RSC Adv.*, vol. 5, no. 13, pp. 9819–9827, 2015.

[10] B. N. Pal *et al.*, "'Giant' CdSe/CdS core/shell nanocrystal quantum dots as efficient electroluminescent materials: Strong influence of shell thickness on light-emitting diode performance," *Nano Lett.*, vol. 12, no. 1, pp. 331–336, 2012.

[11] Y. Kim *et al.*, "Increased shell thickness in indium phosphide multishell quantum dots leading to efficiency and stability enhancement in light-emitting diodes," *Opt. Mater. Exp.*, vol. 4, no. 7, pp. 1436–1443, Jul. 2014.

[12] J. Lee *et al.*, "Direct evidence of n-type doping in organic light-emitting devices: N free Cs doping from CsN_3," *Appl. Phys. Lett.*, vol. 100, no. 20, p. 203301, 2012.

[13] J. Huang, Z. Xu, and Y. Yang, "Low-work-function surface formed by solution-processed and thermally deposited nanoscale layers of cesium carbonate," *Adv. Funct. Mater.*, vol. 17, no. 12, pp. 1966–1973, Aug. 2007.

[14] K. S. Yook *et al.*, "Highly efficient p-i-n and tandem organic light-emitting devices using an air-stable and low-temperature-evaporable metal azide as an n-dopant," *Adv. Funct. Mater.*, vol. 20, no. 11, pp. 1797–1802, May 2010.

[15] P. Piromreun, H. Oh, Y. Shen, G. Malliaras, J. C. Scott, and P. J. Brock, "Role of CsF on electron injection into a conjugated polymer," *Appl. Phys. Lett.*, vol. 77, no. 15, pp. 2403–2405, Oct. 2000.